NIH Public Access
Author Manuscript
Clin Cancer Res. Author manuscript; available in PMC 2013 January 09.

Published in final edited form as:
Clin Cancer Res. 2010 November 15; 16(22): 5390–5401. doi:10.1158/1078-0432.CCR-10-1461.

Hypoexpression and Epigenetic Regulation of Candidate Tumor Suppressor Gene *CADM-2* in Human Prostate Cancer

Guimin Chang[1], **Shuping Xu**[1], **Rajiv Dhir**[2], **Uma Chandran**[2], **Denise O'Keefe**[1], **Norman M. Greenberg**, and **Jeffrey R. Gingrich**[1]

[1]Department of Urology, University of Pittsburgh, Pittsburgh, PA15232

[2]Department of Pathology, University of Pittsburgh, Pittsburgh, PA15232

Abstract

PURPOSE—Cell Adhesion Molecules (CADMs) family comprise a newly identified protein family whose functions include cell polarity maintenance and tumor suppression. *CADM-1*, *CADM-3* and *CADM-4* have been shown to act as tumor suppressor genes in multiple cancers including prostate cancer. However, *CADM-2* expression has not been determined in prostate cancer.

EXPERIMENTAL DESIGN—*CADM-2* gene was cloned and characterized and its expression in human prostatic cell lines and cancer specimens was analyzed by RT-PCR and an immunohistochemical tissue array respectively. Effects of adenovirus-mediated CADM-2 expression on prostate cancer cells were also investigated. *CADM-2* promoter methylation was evaluated by bisulfite sequencing and methylation-specific PCR (MSP).

RESULTS—We report the initial characterization of *CADM-2* isoforms: *CADM-2a* and *CADM-2b,* each with separate promoters, in human chromosome 3p12.1. Prostate cancer cell lines LNCaP and DU145 expressed negligible *CADM-2a* relative to primary prostate tissue and cell lines RWPE-1 and PPC-1 while *CADM-2b* was maintained. Tissue array results from clinical specimens using immunohistochemistry demonstrated statistically significant decreased expression in prostate carcinoma compared to normal donor prostate, benign prostatic hyperplasia, prostatic intraepithelial neoplasia (PIN), and normal tissue adjacent to tumor ($P<0.001$). Adenovirus-mediated CADM-2a expression suppressed DU145 cell proliferation *in vitro* and colony formation in soft agar. The decrease in *CADM-2*a mRNA in cancer cell lines correlated with promoter region hypermethylation as determined by bisulfite sequencing and MSP. Accordingly, treatment of cells with the demethylating agent 5-aza-2′-deoxycytidine alone or in combination with the histone deacetylase inhibitor Trichostatin A resulted in reactivation of *CADM-2a* expression.

CONCLUSIONS—CADM-2 protein expression is significantly reduced in prostate cancer. Its expression is regulated in part by promoter methylation and implicates *CADM-2* as a previously unrecognized tumor suppressor gene in a proportion of human prostate cancers.

Keywords

CADM-2; prostate cancer; methylation; tumor suppressor

Correspondence: Jeffrey R. Gingrich, MD, University of Pittsburgh, Department of Urology, 5200 Centre Ave., Suite 209, Pittsburgh, PA 15232. Tel: 412-605-3015, Fax: 412-604-3030, gingrichjr@upmc.edu.

$watermark-text
$watermark-text
$watermark-text

$watermark-text

$watermark-text

$watermark-text

Introduction

Prostate cancer is the most common malignancy detected in men in the United States and the second leading cause of cancer mortality today (1). The molecular mechanisms underlying progression prostate cancer remain poorly understood, particularly due to the extreme heterogeneity of primary tumors. However, the shift in balance between tumor suppressor genes and oncogenes likely drives both the genesis and progression of this disease. Earlier studies have shown that loss of heterozygosity (*LOH*), mutation, and gene promoter methylation all contribute to the inactivation of tumor suppressor genes in prostate cancer (2). DNA methylation abnormalities, however, have emerged as the most frequent molecular changes in prostate neoplasms (3) such that many tumor suppressor genes undergo CpG hypermethylation and subsequent loss of expression. Examples include the *APC* gene (4), the *CD44* gene (5) and the *E-cadherin* (*CDH1*) gene (6).

Recent studies suggest that cell adhesion molecules (CADM), a newly identified family of proteins, may serve as tumor suppressors (7). Most of the CADMs belong to immunoglobulin superfamily whose members express three extracellular Ig-like loops, a transmembrane region, and an intracellular domain. Multiple normal tissues express CADMs. However, a variety of cancerous tissues either lack CADMs or express them at reduced levels. For example, transcriptional silencing of the *CADM-1* (aliases: *Necl-2/TSLC1/SynCam1/IGSF-4A*) gene occurs in lung cancer (8), prostate cancer (9), and esophageal cancer (10) as a result of promoter methylation. Fukuhara and colleagues reported that the upstream regions of the *CADM-3* (*Necl-1/TSLL1/SynCam-3/IGSF4B*) and *CADM-4* (*Necl-4/TSLL2/SynCam4/IGSF4C*) genes consist of areas rich in guanine and cytosine residues that meet the criteria of CpG islands, suggesting that the promoters of *CADM*-3 and 4 may also undergo methylation (11). A recent study demonstrated a decrease in CADM-4 protein expression in prostate tumors as compared with normal prostate tissue, with evidence suggesting that CADM-4 may suppress tumorigenicity (12). Most recently, many papers have been published to report that CADM-3 and CADM-4 also function as tumor suppressor in multiple cancer cells (13–16), and CADM1 also regulate epidermal adhesion and wound healing and is involved in epithelial cell structure (17–18).

In these studies, we report our analysis of *CADM-2* in prostate cancer, a member of CADM family which has not been previously well characterized in cancer. The gene is also called Necl-3, IGSF4D and SynCAM 2 respectively (19–20) and maps to chromosome 3p12.1, a region which interestingly has been shown to undergo loss of heterozygosity in 56 % of prostate tumors using microarray analysis (21). Most recently, CADM-2 has been characterized as a bona fide adhesion molecule that engages in homo- and heterophilic interactions with the other CADM family members, leading to cell aggregation, and organize functional synapses through heterophilic adhesion. Other reports have shown that CADM-2 is expressed in the nervous system of developing zebra fish (22), suggesting that CADM-2 is a conserved gene evolutionarily and may be implicated in a multitude of physiological and pathological processes. However, so far there is no report about the function of CADM-2 in human cancer cells. In this report, we show that expression of CADM-2 in human prostate cell lines and patient specimens is also reduced as a result of its promoter hypermethylation, implicating *CADM-2* as a tumor suppressor gene in prostate cancer.

Materials and Methods

Cloning of *CADM-2*

By searching the expressed sequence tags (EST) database, dBEST, we found an EST homologous to the *CADM*s. The human EST, from a multiple sclerosis lesion (N77591.1

$watermark-text

$watermark-text

$watermark-text

cDNA clone IMAGE: 290370) was sequenced, which allowed for the identification of a partial open reading frame and subsequent synthesis of gene specific primers for 5′-Rapid Amplification of cDNA ENDs (5′ RACE) to determine the remaining sequence. The full length *CADM-2b* cDNA was obtained by RT-PCR using total RNA extracted from the human prostate. *CADM-2*a and its splice variants were cloned from human prostate and brain respectively using RT-PCR based on the sequences in GenBank (AL834270).

RNA isolation and RT-PCR

Total RNAs from cells were isolated using a rapid guanidine thiocyanate based solution method (RNAzol, Biotecz, Houston, TX). Human adult prostate and brain RNA libraries were purchased from Clontech (Palo Alto, CA). Reverse transcription (RT)-PCR analysis was performed using primers specific for each *CADM-2* isoform: *CADM-2a* upstream primer 5′-CCGCGGATCCACCATGTTTGTTCTCTTCTTGTGCAAC-3′ and downstream primer, 5′-GGAATTCCACAGGTGTACTG-3′-360 base pair product; *CADM-2b* upstream primer 5′-CGGAATTCCGACCATGATTTGGAAACGCAGCGCCGTTCTC-3′ and downstream primer 5′-GGAATTCCATGGTCAGGGCCATT-3′-1 kb product. RT-PCR was performed using a one-step RT-PCR kit (Invitrogen, Carlsbad, CA) with 1 μg of brain or prostate RNA. Reverse transcription was carried out at 55°C for 30 min. After incubation for 4 min at 95°C, PCR was performed for 1 min at 95°C, 1 min at 56°C, and 1.5 min at 72°C for 40 cycles, followed by incubation for 10 min. at 72°C. As a control, *β-actin* was also amplified using the primers 5′-TCCTGTGGCATCCACGAAACT-3′ and 5′-GAAGCATTTGCGGTGGACGAT-3′. Reaction conditions were the same except the PCR went for 20 cycles. The products were subjected to 2% agarose gel electrophoretic analysis.

Recombinant *CADM-2* vectors

CADM-2a-FL, *CADM-2b-FL, CADM-2a-m8* (missing exon 8), and *CADM-2b-m8* (missing exon 8) were cloned into pcDNA3 (Invitrogen) and pEGFP-N1 (Clontech) vectors respectively. *CADM-2b* was cloned using CADM-*2*b-f (sense, *EcoRI*), CG*GAATTC*CGACCATGTTTGTTCTCTTCTTG and CADM-2-r, (antisense, *BamHI*), CG*GGATCC*CGAATGAAATACTCTTTTTT. *CADM-2a* was cloned using CADM-2a-f, (sense, *EcoR I*), CG*GAATTC*CGACCATGATTTGGAAA and CADM-2-r, as shown above. A construct replacing the signal peptide of *CADM-2a* with *CADM-2b* was constructed using *CADM-2*b-Sig, CG*GAATTC*CGACCATGTTTGTTCTCTTCTTGTGCAACCTTTCCTTGGTACCAGCG GCC GCTTCAAAGAATAAAGTTAAA and *CADM-2*r with pEGFP-N1-*CADM-2a-m8* as the PCR template. Recombinant pcDNA3- *CADM-2a-8* was constructed by inserting the PCR fragment amplified by the primer set *CADM-2*a-f and *CADM-2*r-*XbaI*, (antisense, *XbaI*), 5′-GC*TCTAGA*GCTTAAATGAAATACTC using pEGFP-N1- *CADM-2a-m8* as a template. The resultant clones were confirmed by sequencing analysis to identify in-frame fusion of cDNA fragments at the C-terminus or N-terminus.

Cell culture

LNCaP, PC-3, RWPE-1, RWPE-2, HEK-293, DU145, PPC-1, Caco-2 and TSU-pr1 cell lines were obtained from the American Type Culture Collection Company (Manassas, VA), PrEC was purchased from Cambrex Bio Science Walkersville, Inc (Walkersville, MD). [BPH-1 cell line was kindly provided by Dr. Changqing Ma (Department of Pathology, University of Pittsburgh)]. Cell lines were propagated in RPMI 1640 (Gibco Life Technologies, Inc.) containing 10% fetal bovine serum (FBS, Bio-Whittaker, Walkersville, MD) while the HEK-293 cell line was cultured in DMEM containing 10% FBS. RWPE-1 and 2 were maintained in unfiltered Keratinocyte-Serum Free media supplemented with 5 ng/ml human recombinant EGF and 0.05 mg/ml bovine pituitary extract. PrEC cells were maintained in PrEGM™ BulletKit media (Cambrex Bio Science Walkersville, Inc,

$watermark-text

$watermark-text

$watermark-text

Walkersville, MD). All media contained 100 units/ml penicillin and 100 μg/ml streptomycin (Invitrogen). Cells were grown in 5% CO_2 at 37°C.

Peptides synthesis and antibody generation

Synthetic peptides corresponding to the following hydrophilic segments of CADM-2 were produced: N-term (CADM-2a, 165–183), C-term (CADM-2a, 426–444) CIINAEGSQVNAEEKKEYFI. After conjugation to keyhole limpet hemocyanin (KLH), peptides were injected into rabbits and boosted twice; resulting anti-peptide antibodies were affinity purified by using the immunizing peptide (Research Genetics, Inc. Huntsville, AL). RP-conjugated goat anti-rabbit IgG (Santa Cruz, CA) were used as a secondary antibody for immunofluorescence staining. Mouse monoclonal antibodies against GFP and human α-tublin and goat monoclonal antibody against human β-actin were obtained from Santa Cruz Biotechnology (Santa Cruz, CA).

Construction of recombinant adenoviruses and transduction of adenovirus on prostate cancer cells

Recombinant adenovirus was generated by AdEasy system as described previously (23). Wild-type *CADM-2a* full-length and missing exon 8 variant cDNA were cloned into the shuttle plasmid pAdTrack-CMV vector (this vector contains a GFP expressed cascade for monitoring gene expression) available from the ATCC. The sequenced and purified pAdTrack-CMV- CADM-2plasmids and the Ad genomic plasmid pAD-Easy (delta) E1, E3 Cre were cotransfected into *E. coli* cells for site-specific recombination. Recombinant vector was transfected into 293 cells and positive adenovirus plaque was purified with agarose overlay, AdTrack-CMV with no transgene insertion as control. The recombinant adenovirus Ad-CADM-2 was used after purification, characterization, and titration of the viral infectivity by fluorescence assay. Adenoviral mediated transduction of DU145 was performed as stated previously (24). Briefly, DU145 was infected with control virus AdCMV, Ad-CADM-2 or Ad- CADM-2-m8 *in vitro* at serial MOIs. After viral infection, cells were incubated at 37°C, and cells were harvested 24 hours after viral infection for western blot detection.

Transient transfections and Western blot analysis

Cells were transiently transfected with recombinant pcDNA3 constructs of the *CADM-2* isoforms or the corresponding empty vector as the control, using LipofectAMINE plus reagent (Invitrogen) for 4 hours. For Western blots, 5×10^6 transfected cells/well were washed three times with ice-cold PBS 48 h post-transfection and suspended in 250 μl of ice-cold lysis buffer containing protease inhibitor mixture. Human prostate and brain protein medleys were purchased from BD bioscience (Palo Alto, CA). Samples were run on 10~12 % SDS-PAGE acrylamide gels and transferred. Blots were incubated with the primary antibodies for 60 min at room temperature. After incubation with the appropriate secondary antibody, bands were visualized using an ECL detection system or Pierce sepersignal system (Pierce Biotechnology, Inc., Rockford, IL).

Adenoviral transduction for *in Vitro* Studies

DU145 was infected with control virus Ad-CMV, Ad-*CADM*-2a-m8 and Ad-*CADM*-2a-FL *in vitro* at a MOI of 5 or 20. After viral infection, cells were incubated at 37°C, and cell lysates were harvested for Western blot assay and peptide competition assay.

Antibody specificity determination by peptide competition assay

To determine whether the binding of C- term antibody was specific for the CADM-2 protein, a peptide competition assay was performed according to previous report (25).

$watermark-text

$watermark-text

$watermark-text

Essentially, this assay is a modified Western blot in which a competing pre-incubated mixture of C-term antibody together with the peptide is substituted for the primary antibody. Rabit anti-human CADM-2 C-term antibody diluted 1:2000 (1 μg/ml) in 5% (w/v) BSA/TBST was pre-incubated 1 h at room tempeture in a solution containing a serial diluted concentration (0, 1ng/ml, 10 ng/ml, 0.1 μg/ml, 1 μg/ml, 10 μg/ml) of the competing C-term homologous peptide, the diluted N-term peptide was used as negative control. These mixtures were centrifuged at 20,000 *g* for 15 min, and the supernatants were applied onto a nitrocellulose membrane to which the 293 cell lysate or DU145 cell extracts transduced by Ad-*CADM*-2a-FL or Ad-*CADM*-2a-m8 at different MOIs had been transblotted. Subsequent steps were identical to the Western blotting previously described.

Patient material and tissue microarray construction

A tissue array from 176 patients underlying surgery from 1996~2003 representing different stage and grade of prostate cancer was utilized to evaluate the CADM-2 expression (26). Multiple replicate core samples of normal, high-grade prostatic intraepithelial neoplasia (PIN), and prostate cancer tissue were acquired from each case. The TMA set included progression TMAs (109 cases of prostate cancer with different Gleason grades and prostate cancer T stage). The TMAs also contained foci of metastatic prostate cancer, PIN, normal adjacent to tumor (NAT), benign prostatic hyperplasia (BPH), and “true normal” prostatic tissue from organ donors (see Table).

Immunohistochemistry

Tissue microarray slides were stained for CADM-2 expression using a polyclonal antibody directed against C-terminus of CADM-2 as stated above. Tissue microarray slides were soaked overnight in xylene. The following day, the slides were cleared in two fresh changes of xylene for 20 minutes each, hydrated in two changes of 100% ethanol for 20 minutes each, one change of 95% ethanol for 20 minutes, and one change of 70% ethanol for 20 minutes. Slides were then rinsed in several changes of distilled water. Slides were placed in a working solution of TBS buffer for 5 minutes before loading onto an Autostainer. Once on the Autostainer, slides were blocked with peroxidase for 5 minutes and then rinsed with TBS buffer. After proteinase K treatment for 8 minutes, the slides were rinsed with TBS buffer, incubated with CADM-2 C-term primary antibody (1:1000) for 30 minutes, and then rinsed again with TBS buffer. The slides were incubated with mouse labeled polymer for 30 minutes and then rinsed with TBS buffer followed by incubation with DAB and chromogen for 10 minutes and then rinsing with distilled water. The slides were then counterstained with Dako-Hematoxylin for 1.5 minutes and washed with warm tap water for 2 minutes before being dehydrated, cleared, and cover-slipped.

Immunohistochemical tissue microarry analysis

Tissue microarray data sets consisted of 647 tissue samples from 176 different patients with ages ranging from 15 to 85 years (Table). Immunohistochemical staining was scored from 0 to 4 depending upon the amount of staining present. The analysis scale was based on percentage of cells with whole cell positivity. The scale used was 0 = no expression; 1 = cell positivity seen in up to 10% of cells; 2 = cell positivity seen in 10% to 25% of cells; 3 = cell positivity seen in 25% to 50% of cells; 4 = cell positivity seen in more than 50% of cells. For all high IHC scores, a cutoff of 3 or more was used. Because one patient was used for more than one tissue sample and these tissue samples were correlated, the values of these tissue samples on each slide were averaged. There were 11 donors, 17 benign tissues (BPH), 38 high-grade PIN, 42 NAT, 109 prostate adenocarcinoma (PRCA), 6 metastatic lymph node tissues, and 10 metastatic tissues. Mean values from each group were compared between prostate tissue groups using the Mann-Whitney rank sum test and *P* values of less than .05 were considered significantly different. Kruskal-Wallis 1-way analysis of variance

$watermark-text

$watermark-text

$watermark-text

on ranks compared mean values within Gleason scores and stages of prostate cancer. *P* values of less than .05 were considered significant. All pairwise multiple comparison procedures were conducted using Dunn method.

In vitro proliferation assay and colony formation in soft agar

DU145 cells grown on 24-well plates to about 50% confluence were infected with Ad-*CADM-2*a-m8, Ad-*CADM-2*a-FL and Ad-CMV viruses at MOIs of 10, 20 and 50 MOI/cell. The cell numbers were determined by MTT assay after 3 and 5 days of infection.

DU145 cells were grown to 50–70% confluence. Cells were transduced with the Ad-*CADM-2*a-m8, Ad- *CADM-2*a-FL and Ad-CMV viruses respectively at MOIs of 5 MOI per cell. After 48h, cells were trypsinized and anchorage-independent cell growth was assayed in soft agar (27). Briefly, 6-well plates were coated first with 3 ml bottom agar (DMEM, 10% FBS, 0.6% agar), and then with 2 ml top agar (DMEM, 10% FBS, 0.3% agar) containing 1×10^4 cells transiently transducted by three kind of adenoviruses. Every 3 days, normal growth medium was gently layered over the cultures. Colony formation was monitored daily by light microscopy. Colonies in soft agar were counted after 15 days using an IMT-2 inverted research microscope (Olympus, Japan).

Bisulfite sequencing methylation analysis

Bisulfite sequencing and T-A cloning were performed as previously described (9, 28). Briefly, genomic DNA was extracted from cells by DNA-Bee reagent (TEL-TEST Inc., Friendswood, TX) and purified with the QIAamp DNA kit (Qiagen, Valencia, CA). DNA was denatured with 0.3 M NaOH for 15 minutes at 37°C, followed by treatment with 3.1 M sodium bisulfite and 0.8 mM hydroquinone (Sigma, St. Louis, MO), pH 5.0, at 50°C for 16 h. DNA was then treated with 0.2 M NaOH for 10 min at 37°C. The modified DNA was purified using DNA cleanup kit (Promega) in a total volume of 20 μL, and 1 μL was used for genomic sequencing and MSP. Modified DNA (100 ng) was amplified by PCR using primers F1 (sense primer F1 5′-TATTAGTAGGAGGAGGAGGAGAAGAA -3′) and R1 (antisense primer R1 5′-CCCTTCTCTAAAAAACTAAAAAAAA -3′). Primers were based on the Methprimer Program software analysis of the CADM-2*a* promoter to avoid any CpG dinucleotides (15). PCR reaction conditions were as follows: 95°C for 15 min to activate HotStarTaq polymerase; followed by 50 cycles at 94°C for 1 min, 56°C for 1 min and 72°C for 1 min; and a final incubation at 72°C for 10 min, the size of PCR product is 237 bp from -237 bp to start codon ATG. The PCR product was purified and sequenced. To confirm the efficiency of the bisulfite reaction, 10 non-CpG cytosine residues were evaluated for conversion to uracil residues, and repeated independently three times. To quantitatate the methylation rate of CpG sites in specific cells, the PCR product was cloned into pCR2.1-TA cloning vector (Invitrogen); 6 positive clones were picked from each cell line for sequencing.

Methylation-specific PCR (MSP) analysis

Genomic DNA (100 ng) from all prostate cells and tissues was subjected to sodium bisulfite modification is stated above. Based on the promoter sequence of *CADM*-2a, MSP and unmethylation-specific PCR (USP) primers were designed using Serologicals CpGware software (https://apps.serologicals.com/cpgware/dna_form2.html). Primers used for MSP and USP analysis are as follows: MSP primers, 5′-ATCTATCCCTAACCGAAATAAAAACGAAA-3′ (sense), 5′-AAGTAAGTAGTATTGTCGTTCGCGTTC -3′ (antisense); USP primers, 5′-ATATCTATCCCTAACCAAAATAAAAACAAAA-3′ (sense), 5′-AGTAAGTAAGTAGTATTGTTGTTTGTGTTT -3′ (antisense), with a MSP and USP product size of 251 bp and 256 bp respectively. The region of *CADM-2a* 5′-UTR from −

$watermark-text

$watermark-text

$watermark-text

442 to −659 was chosen for MSP analysis. The annealing temperature and PCR cycles used for MSP and USP primers were 60°C and 50 cycles, respectively. MSP analysis of human specimens was performed according to a previous reports (29). DNA isolated from tissue sections was subjected to bisulfite conversion using the EZ DNA Methylation Kit (Zymo Research) according to the manufacturer's directions. Primers for MSP were: CADM-2 Meth F2 (sense), 5′-TTTTGCGGGTGTTTTGTC-3′ and CADM-2 METH R (anti-sense), 5′-TAATATCCTCCTCCCGACG-3′. Bisulfite modified DNA was amplified by PCR. The condition of the MSP was as follows: 94 °C for 10 min for denaturation, 40 cycles of amplification (94 °C, 30 sec; 53 °C, 30 sec; 72 °C, 30 sec) with a final elongation step of 10 min at 72 °C. In each assay, the absence of DNA template served as a negative control. The obtained MSP and USP products were analyzed by electrophoresis in non-denaturing 8 % polyacrylamide gels stained with ethidium bromide. DNA from human genomic DNA (Chemicon International Inc., Temecula, CA) was bisulfite converted and used as a positive control for unmethylated genes. DNA from a primary human fetal cell line (Chemicon International Inc.) treated *in vitro* with M.*Sss*I bacterial CpG methylase (New England Biolabs Inc., Beverly, MA) was bisulfite converted and used as a positive control for methylated alleles.

Demethylation analysis

PC-3, DU145, LNCaP, and TSU- Pr1 cells were plated at 10^6 per 100 mm dish and grown for 24 h. 5-aza-dC (Sigma) was added daily for 4 days at concentrations of 0, 2.5 or 5 μM. The cases in which cells were cultured with both TSA (Cayman Chemical Company, Ann Arbor, Michigan) and 5-aza-dC, cells were initially treated with 5-aza-dC for 72 h followed by an additional dose of 5-aza-dC, and then TSA 8h later. TSA concentrations ranged from 6.5 to 150 ng/ml. Cells were incubated for a maximum of 16 h before harvesting (3.5×10^6 cells/dish). Total RNA was extracted using the RNA-Bee isolation kit and reverse transcribed using the superscript one step RT-PCR system (Invitrogen). The reaction was incubated at 94°C for 5 min, followed by 50 cycles (TSU-pr1 cells) or 40 cycles (PPC-1, DU145 and LNCaP cells) at 94°C for 30s, 56°C for 30s, and 72°C for 45s, using forward primer (5′-ACCATGATTTGGAAACGCAG-3′) and reverse primer (5′-GGAATTCCACAGGTGTACTG-3′) for a 365 kb product. β-actin served as a control.

Results

Cloning and characterization of CADM-2

The full-length cDNA clone of *CADM-2* was obtained by RT-PCR using total RNA extracted from the human prostate. Analysis of the sequence revealed a predicted open reading frame of 1311bp and a 437 amino acid protein with an estimated molecular weight of 47.7 kDa. A high degree of homology of peptides exists between CADM-2 and the other CADM proteins: human CADM-3 (Necl-1/human TSLL1) (44.4% homology), human CADM1 (Necl-2/human IgSF4/TSLC1) (40.8%), and CADM-4 (human Necl-4/human TSLL2) (33%). The mRNA sequence was submitted to GenBank as *CADM-2* (*Necl-3*) under accession number **AF538973.** Database searches identified another mRNA sequence, accession number **AL834270** differing primarily in the amino acids encoding a putative signal peptide (94.7% homology). Searching the human genome database with each signal peptide sequence revealed that each matched separate regions in genomic contig NT_022459.12 of chromosome 3p12.1, suggesting the existence of two isoforms designated *CADM-2a* and *CADM-2b* respectively. In addition to divergent signal peptides, analysis revealed other differences between *CADM-2a* and *CADM-2b* (Figure 1A). *CADM-2a* includes 27 bp found in the 3′ end of the first exon of *CADM-2b,* designated exon V1b. Furthermore, the isoforms have different start codons, indicating that they have different

promoters. The *CADM-2b* promoter appears to reside in the intron between exons 1a and 1b.

Putative domains of CADM-2

Domain analysis was performed by Simple Modular Architecture Research Tool (SMART) software and transmembrane segments TMHMM2 software, and demonstrated that CADM-2 has a predicted extracellular (EC) domain containing one Ig-like V–type loop and two Ig-like C2-type loops, a single hydrophobic trans-membrane domain, and a short intracellular (IC) domain containing a protein 4.1-binding motif and a terminal PDZ-binding motif (Figure 1B). The EC domain of CADM-2a bears six N*X*(S/T) motifs for *N*-linked glycosylation and one proximal membrane *O*-glycosylation site predicted by website-based software NetOGlyc 3.1.

Splice variants of CADM-2

Forward primers designed to hybridize to the first exon sequence of either *CADM-2a* or *CADM-2b* and a reverse primer incorporating the stop codon were used to amplify both isoforms from whole brain and total prostate RNA. Prostate and brain tissue expressed both *CADM-2a* and *CADM-2b*, while only prostate expressed an isoform of *CADM-2*a lacking the sequence for 41 amino acids in the membrane-proximal region which includes a putative *O*-glycosylation site. This sequence region corresponds to exon 8 as determined by the Genescan program. This isoform missing exon 8 has been designated *CADM-2a-m8*.

Expression patterns of *CADM-2*a and *CADM-2*b mRNA and protein in prostate cancer cell lines

Expression of *CADM-2a* and *CADM-2b* was evaluated by RT-PCR in various prostate cancer cell lines, in the bladder cancer cell line TSU-pr1, and in the “normal” prostate cell line RWPE-1 which has been immortalized by HPV18. Normal brain and prostate tissues were also examined. Non-quantitative PCR demonstrated relatively uniform *CADM-2b* mRNA expression in all cell lines and tissues examined (Figure 2A). In contrast, *CADM-2a* mRNA varied substantially with the highest levels in normal brain and prostate tissue, PPC-1 cells and RWPE-1 cells. The metastatic prostate cancer cell lines PC3, LNCaP and DU145 as well as metastatic TSU-pr1 cells had low or nearly absent levels of *CADM-2a* mRNA. RWPE-2 cells, a tumorigenic derivative of RWPE-1 cells transformed by K-ras, also displayed decreased levels of *CADM-2a* mRNA (Figure 2A). We noted the presence of two distinct *CADM-2a* bands in normal prostate tissue. Sequencing results demonstrated that the two bands represented *CADM-2a* and *CADM-2*a*-m8*.

To determine endogenous expression of CADM-2 in several cell lines, we developed two peptide antibodies: N-term and C-term. The presence of CADM-2 in cell lines was determined using two affinity-purified polyclonal antibodies respectively. The predicted molecular weight of endogenous CADM-2 is about 50 kDa. Mutiple non-specific bands were detected by N-term antibody in all cell lines and tissues (data not shown), indicating that the N-term antibody was not specific. CADM-2 protein expression in HEK-293, Caco-2 cell lines (Fig. 2B) detected by C-term antibody was quite high, while significantly less in all “normal” prostate cell and cancer cell lines (Fig. 2B). CADM-2 expression in HEK293 and Caco-2 showed a single clear band with double protein size when compared with that in mouse liver suggestive of probable dimerization which may be SDS-resistant (Fig. 2B). We used mouse liver extract as positive control as mouse *CADM-2* has a similar C-terminus sequence to human *CADM-2*.

CADM-2 mRNA was highly expressed in the “Normal” prostate cell line such RWPE-1, primary prostate cancer cell line PPC-1 and normal prostate tissue, but reduced or even lost

$watermark-text $watermark-text $watermark-text

$watermark-text

$watermark-text

$watermark-text

in several prostate cancer cell lines. Protein expression was lost in all prostate cell lines tested only detectable in Caco-2 (a polarized cell line) and HEK-293 (Human embryonic kidney cell line), suggesting that CADM-2 protein may be either cleaved or degraded when prostate cells become transformed or immortalized, but stably maintained in cells with high polarity and adhesion, suggesting that CADM-2 may be involved in maintenance of cell polarity and cell adhesion.

Differential processing of the CADM-2 isoforms

CADM-2 cDNA isoforms were cloned into the pN1 plasmid to express fusion proteins including an N-terminal enhanced green fluorescent protein (EGFP). Transfection of HEK 293 cells with pEGFP-N1 vector alone yielded a 30 kDa band as predicted (Figure 3A). Western analysis of cells transfected with pN1-*CADM-2a-m8* and pN1-*CADM-2a* revealed robust bands at 80 to 86 kDa. The sizes of these bands exceeded the predicted size of 75 kDa for CADM-2a-m8-EGFP and 78 kDa for CADM-2a-EGFP, suggesting possible glycosylation of the six putative *NXS/T* N-glycosylation sites. Indeed, when digested with the enzyme PNGase F, the detected bands decreased to the predicted size (data not shown), confirming the presence of *N*-glycosylation. In contrast, transfection of pN1-*CADM-2b* yielded only a weak band at 30 kDa consistent with protein degradation. Therefore, to determine whether the different signal peptides result in differential processing of CADM-2, the signal peptide of *CADM-2a-m8* was replaced with the signal peptide from *CADM-2b*, creating *CADM-2b-m8.* Transient transfection with pN1-*CADM-2b-m8* resulted in a very weak band at 80 kDa, the predicted size for the fusion protein, as well as the 30 kDa band size for EGFP, confirming that the CADM-2b signal peptide results in protein degradation. More interestingly, there are some small bands detected by GFP antibody especially *CADM-2*a isoforms (Figure 3A), suggesting that CADM-2-GFP fusion protein may be cleaved by some specific enzymes. Detailed mechanisms warrant further investigation.

Determination of CADM-2 antibody specificity using peptide competition assay

To further test the specificity of anti-CADM-2 antibodies, several peptide competition assays were performed. We utilized exogenous adenoviral mediated CADM-2a-m8 protein in DU145 cells and endogenous CADM-2 in 293 cells for peptide competition assay. Fig. 3B shows that the protein amount of both CADM-2a full length and CADM-2a-m8 expression increased with the higher adenoviral multiple of infections (MOIs). However, the expression pattern of the two vectors was different with the bands of CADM-2a-m8 broad range from 50 ~ 100 kDa due to *N*-glycosylation (data not shown). CADM-2a had two isolated major bands, possibly due to *O*-glycosylation modification, as CADM-2a-m8 is missing exon 8, which encodes potential *O*-glycosylation site. The peptide competition assay generated similar results between ectopic CADM-2 expression at 5 MOI adenoviral mediated *CADM-2a-m8* in DU145 cells (Fig. 3C) and endogenous 293 cells (Fig. 3D). The density of CADM-2 band detected by C-term antibody, 110 kDa in 293 and 55 kDa in Ad-CADM-2a-m8 respectively, was reduced with the increase of homologous C-term peptide even was absent with increase of C-term peptide up to 10 μg/ml concentration, indicating that the homologous C-term peptide inhibited binding. As expected, under identical conditions, heterologous N-term peptide did not block the binding of C-term antibody, suggesting no competitive inhibition by the N-term peptide. Thus the specificity of anti-CADM-2 C-term antibody was comfirmed.

CADM-2 expression in normal tissue and human prostate cancer specimens

No significant CADM-2 protein expression in prostate cell lines prompted us to determine if expression could be detected in human normal tissues. Results showed that CADM-2 protein was highly expressed in normal brain and prostate (Fig. 4A). C-term antibody reacted with multiple protein bands detected in brain and prostate tissue (Fig. 4A). The multiple bands

$watermark-text

$watermark-text

$watermark-text

may be due to complex *N*- and/or *O*- glycosylation, since five potential *X*(S/T) motifs for *N*-linked glycosylation, and one potential proximal *O*-glycosylation sites were predicted by the software stated above (data not shown).

To further evaluate CADM-2 protein expression, prostate tumor tissue micro arrays were examined. Immunohistochemical analysis revealed that adenocarcinoma exhibits significantly lower levels of CADM-2 protein than normal adjacent tissue, benign prostatic hyperplasia (BPH), PIN and normal donor tissue (Fig. 4B and Table 2). However, when CADM-2 expression was analyzed according to stage and Gleason score, there was no significant difference of CADM-2 by pathological stage, indicating that CADM-2 expression is reduced or lost during prostate carcinogenesis. Evaluation of CADM-2 levels according to Gleason scores revealed that the differences in the median values among the various scoring groups lacked statistical significance and thus differences may have resulted from random sampling variability.

Ectopic expression of CADM-2a suppresses DU145 cell proliferation

To investigate whether CADM-2a effects prostate cell proliferation, DU145 cells were transiently transduced with Ad-*CADM*-2a-FL, Ad-*CADM*-2a -m8 and Ad-CMV respectively. The number of viable cells at 3 and 5 days after transduction with adenoviruses at various MOIs was determined by the MTT assay. The viability of transduced cells was compared with that of untransduced DMEM-treated control cells. The results presented in Figure 5A demonstrate that cell viability was markedly reduced for DU145 cells transduced by Ad-*CADM*-2a-FL, Ad-*CADM*-2a -m8 respectively at both time point and inhibition of cell viability is dose-dependent. Additionally, after 5 days of transduction at 50 MOI, both Ad-*CADM*-2a-FL and Ad-*CADM*-2a -m8 killed almost 84% of Du145 cells. In contrast, the growth of cells treated with control virus containing no inserts, Ad-CMV, was only slightly affected. There are significant difference between Ad-*CADM*-2a-FL or Ad-*CADM*-2a -m8 group and control viral group Ad-CMV at day 3 and day 5 post-transduction respectively ($P < 0.01$). The mechanisms of this inhibition warrant further investigation.

Effect of CADM-2a on colony formation in soft agar

Introduction of tumor suppressor genes into tumorigenic cells can reverse the ability of these cells to grow in an anchorage-independent manner (30). Therefore, we assessed whether exogenous CADM-2a impacted anchorage-independent growth in DU145 cells. 1.0×10^4 DU145 cells, transiently transduced by Ad-*CADM*-2a-FL, Ad-*CADM*-2a -m8 and Ad-CMV at 5 MOI respectively, were seeded in soft agar and allowed to grow for 15 days. DU145 parental cells and cells with Ad-CMV vector alone served as control group. Introduction of either the *CADM-2a-m8* or *CADM-2a-FL* by viral vectors significantly decreased the number of colonies able to form in soft agar while compared with DU145 parental cells and cells with Ad-CMV vector alone ($P < 0.01$). This finding combined with the cell proliferation assay suggested that CADM-2 can function as a putative tumor suppressor in prostate cancer.

Bisulfite sequencing analysis of CADM-2a 5′-UTR methylation

According to the RT-PCR analysis, *CADM-2a* RNA expression generally decreased in prostate cancer cell lines compared with more normal prostate cell lines and tissue. Therefore, *CADM-2a* and *CADM-2b* sequences were analyzed by Methprimer Program software for possible methylation sites (31). Based on GC content (64.4%) and the ratio of observed to expected CpG dinucleotides (0.674), the 5′UTR of *CADM-2a* contains two CpG islands: one located between −682 bp and −58 bp relative to start codon ATG and a second one located between −1002 bp and −832 bp. In contrast, the 5′UTR of *CADM-2b* has no putative CpG islands. Note that the identification of the *CADM-2a* promoter and its

$watermark-text

$watermark-text

$watermark-text

first exon in human chromosome 3 was based on the FirstEF program (32). The results of this analysis indicated that the putative transcription start site was 928 bp upstream of the ATG start codon.

Bisulfite genomic sequencing was used to test for *CADM-2a* promoter hypermethylation. Genomic DNA from RWPE-1, RWPE-2, PPC-1, DU145, LNCaP, PC-3 and TSU-pr1 cells was isolated and modified with bisulfite, which converts cytosine residues to uracil while leaving 5-methylcytosine unaltered. From each cell line, a 237 bp fragment spanning −237 bp to 0 bp relative to ATG within the putative CpG island was amplified by PCR, subcloned into a TA vector, and then 6 clones per cell line sequenced. Almost all of the 22 CpG dinucleotides within the fragment were methylated in DU145 (79.5%), LNCaP (71.2%) and TSU-pr1 (82.6%) cells, although methylation was not complete. In contrast, none of the sites in clones from RWPE-1 and PPC-1 DNA exhibited methylation (0%) (Fig. 5A). Interestingly, DNA from PC-3 and RWPE-2 cells displayed more heterogeneity; with the CpGs in some of the clones heavily methylated while other clones were sparsely or totally unmethylated. The overall methylation frequency of DNA from RPWE-2 and PC-3 cells was 61.4% and 43.9% respectively (Figure 6A). There was also a trend of decreasing methylation frequency towards the 3′ end of the CpG islands in many of the cancer cells. Combined with the transcript expression studies, this suggested an inverse relationship between promoter methylation and gene transcription.

MSP analysis of the CADM-2a 5′UTR in prostate cancer cell lines and patient speciments

To confirm the findings in tissue culture cell lines, we used methylation specific PCR (MSP) analysis to further evaluate *CADM-2a* methylation in the cell lines and patient specimens. The MSP analysis corroborated the bisulfite sequencing: the 5′UTR was predominately methylated in LNCaP and DU145 cells; partially methylated in RWPE-2, PC-3 and TSU-pr1 cells; and unmethylated in RWPE-1 and PPC-1 cells (Figure 6B). Methylation of the *CADM-2a* 5′UTR was present in 3 of the 9 patient tumors (Figure 6C). Of note, all 3 tumors positive for MSP were high-grade disease. In addition, of the 4 patients that developed recurrent disease, 2 had tumors with methylated *CADM-2a* (Table 2).

Restoration of CADM-2a expression through treatment with 5-aza-dC and/or TSA

To validate the role of DNA methylation in silencing *CADM-2a*, the ability of the DNA methylation inhibitor 5-aza-2′-deoxycytidine (5-aza-dC) and the histone deacetylase (HDAC) inhibitor Trichostatin A (TSA) to restore *CADM-2a* expression in cell lines was tested. After treatment with 5-aza-dC, expression of *CADM-2a* mRNA in PPC-1 cells remained consistent while expression was restored in a dose-dependent manner in LNCaP cells (Figures 6D-a and -b). While 5-aza-dC weakly reactivated *CADM-2a* expression in DU145 cells, it had no effect on expression in TSU-pr1 cells. The combination of 5-aza-dC with TSA demonstrated reactivation of gene expression levels in DU145 and TSU-pr1 cells (Figures 6D-c and -d). These data suggest that repression of *CADM-2a* expression occurs, at least in part, through *CADM-2a* hypermethylation as well as histone deacetylation.

Discussion

The CADM family is a recently described family of genes whose protein expression and function has not been completely characterized. We cloned *CADM-2* from normal prostate to assess any potential role that this gene may have in the development and progression of prostate cancer. We have shown that the *CADM-2* gene encodes two isoforms, *CADM-2a* and *CADM-2b*, each driven by an independent promoter. *CADM-2a* and *CADM-2b* differ primarily in signaling peptides, likely resulting in differential cellular localization, cell

$watermark-text

$watermark-text

$watermark-text

processing and potentially in function. We have been unable to detect or demonstrate stable *CADM-2b* protein expression in spite of clear mRNA expression.

Prostate and bladder cancer cell lines obtained from metastases such as DU145, PC-3, LNCaP and TSU-pr1 cells, demonstrate decreased levels of *CADM-2a mRNA* compared with levels in RWPE-1 cells, and normal prostate and brain tissues. This finding correlates with hypermethylation of the promoter, suggesting that silencing of CADM-2a may be an important event in the development or the progression prostate cancer. RWPE-2 cells, the tumorigenic derivative of RWPE-1 cells transformed by K-ras and PPC-1, also expressed diminished levels of *CADM-2a* mRNA. In contrast, *CADM-2b* mRNA levels remained relatively similar in all cell types examined. Differential regulation through hypermethylation of the *CADM-2a* promoter likely accounts for this difference in expression pattern Interestingly, *CADM-2a* expression in RWPE-2 cells was significantly decreased compared to RWPE-1, implicating a connection between Ki-Ras expression and *CADM-2a* hypermethylation. Indeed, one group reported that activated Ras, in combination with the *SV40* T antigen, immortalized normal human bronchial epithelial cells that then formed colonies in soft agar. The transformation corresponded with high levels of DNA methyltransferase (DNMT3b) activity such that methylation and subsequent silencing of several tumor suppressor genes occurred, including *CADM-1* (33).

CADM-2a expression was restored in selected cell lines after 5-aza-dC and/or TSA treatment, further confirming that hypermethylation is a major mechanism for silencing CADM-2a. 5-aza-dC-mediated inhibition of DNA methyltransferase, which alone maintains the genomic *de novo* methylation of cytosines, was able to induce *CADM-2a* gene expression appreciably in LNCaP cells, but only weakly in DU145 cells and not at all in TSU-pr-1 cells (Figure 6D). TSA treatment of DU145 and TSU-pr1 cells perhaps weakly induced some expression (Figure 6D). Interestingly, a recent report (34) illustrated that TSA can induce DNA demethylation in the absence of 5-aza-dC. However, the combination of TSA and 5-aza-dC synergistically induced *CADM-2a* transcription in both DU145 and TSU-pr1 cells (Figure 6D). The ability of these two inhibitors to work in concert to restore expression has been demonstrated for many genes, including the estrogen receptor (35) and metallothionein 1G (MT1G) (36), and is consistent with the recently uncovered mechanisms by which methylation regulates gene expression.

To understand the mechanism by which this down-regulation occurs in adenocarcinoma of the prostate, we have investigated CADM-2 expression by immunohistochemical staining. Using prostate TMA slides, we show a significant down-regulation of CADM-2 in PCa that does not correlate with tumor grade and progression in our prostate TMAs. Except CADM-3 which is highly expressed in neural system, all CADM molecules are expressed in multiple tissues including prostate. Accordingly, loss of expression of Necl-2 in PPC-1 is due to its promoter methylation. Bisulfite sequencing assay determined that promoter methylation was found in 32% primary prostate tumors, and showed no significant association with the Gleason score and TNM staging (9). In one report (37), using a tissue microarray and immunohistochemical staining, the frequency of down-regulated or lost expression of CADM-1 in metastatic nasopharyngeal carcinoma (NPC) lymph node was significantly higher than that in primary NPC, suggesting that *CADM-1* is a tumor suppressor gene in NPC. CADM-4 (Necl-4/IGSF4C) is mainly expressed in the prostate, kidney, bladder in addition to the brain according to one report. Its expression is reduced or lost in prostate cancer cell lines such as PPC-1 and DU145. Introduction of CADM-4 into PPC-1 strongly suppresses subcutaneous tumor formation in nude mice (12). These findings indicate that alteration of these three CADMs is associated with prostate tumor genesis and/or metastasis.

$watermark-text

$watermark-text

$watermark-text

The increased methylation of *CADM-2a* and subsequent decrease in expression in prostate cancer cells suggests that CADM-2a acts as a novel tumor suppressor, especially given that other CADMs serve as tumor suppressors in a variety of cancers. The ability of cells to grow in an anchorage-independent manner represents a hallmark of tumorigenesis and adenovirus-mediated overexpression of CADM-2A statistically suppressed DU145 cell growth *in vitro*, indicating that restoration of CADM-2 expression attenuates prostate cancer growth functioning like tumor suppressor and ability of CADM-2a to diminish colony formation in soft agar further supports its role as a tumor suppressor (Fig. 5). Mo et al (38) reported that adenovirus-mediated CADM-1 (TSLC1) inhibits non-small-cell lung cancer growth through induction of apoptosis. Detailed mechanisms of CADMs family to suppress tumor growth need to be further investigated.

In conclusion, based on the data in this study, we propose that CADM-2 may act as a tumor suppressor in the progression of transformed prostate cancer cells to invasive and metastatic prostate cancer. Moreover, the silencing of CADM-2a is accomplished at least in part through promoter hypermethylation and may be associated with more aggressive prostate cancer. These conclusions warrant confirmatory investigations in a larger number of patients over a wider spectrum of disease. In addition, they suggest that understanding the biologic function of CADM-2 may lead to further insights into the development and progression of prostate cancer, as well as potential therapeutic targets.

Acknowledgments

We would like to thank Moira Hitchens for her valuable comments and critical review of this manuscript.

References

1. Jemal A, Siegel R, Ward E, Hao Y, Xu J, Thun MJ. Cancer statistics, 2009. CA Cancer J Clin. 2009; 59:225–49. [PubMed: 19474385]
2. Simard J, Dumont M, Labuda D, et al. Prostate cancer susceptibility genes: lessons learned and challenges posed. Endocr Relat Cancer. 2003; 10:225–59. [PubMed: 12790786]
3. Schulz WA. DNA methylation in urological malignancies (review). Int J Oncol. 1998; 13:151–67. [PubMed: 9625817]
4. Kang GH, Lee S, Lee HJ, Hwang KS. Aberrant CpG island hypermethylation of multiple genes in prostate cancer and prostatic intraepithelial neoplasia. J Pathol. 2004; 202:233–40. [PubMed: 14743506]
5. Lou W, Krill D, Dhir R, et al. Methylation of the CD44 metastasis suppressor gene in human prostate cancer. Cancer Res. 1999; 59:2329–31. [PubMed: 10344738]
6. Li LC, Zhao H, Nakajima K, et al. Methylation of the E-cadherin gene promoter correlates with progression of prostate cancer. J Urol. 2001; 166:705–9. [PubMed: 11458121]
7. Takai Y, Irie K, Shimizu K, Sakisaka T, Ikeda W. Nectins and nectin-like molecules: roles in cell adhesion, migration, and polarization. Cancer Sci. 2003; 94:655–67. [PubMed: 12901789]
8. Kuramochi M, Fukuhara H, Nobukuni T, et al. TSLC1 is a tumor-suppressor gene in human non-small-cell lung cancer. Nat Genet. 2001; 27:427–30. [PubMed: 11279526]
9. Fukuhara H, Kuramochi M, Fukami T, et al. Promoter methylation of TSLC1 and tumor suppression by its gene product in human prostate cancer. Jpn J Cancer Res. 2002; 93:605–9. [PubMed: 12079507]
10. Ito T, Shimada Y, Hashimoto Y, et al. Involvement of TSLC1 in progression of esophageal squamous cell carcinoma. Cancer Res. 2003; 63:6320–6. [PubMed: 14559819]
11. Fukuhara H, Kuramochi M, Nobukuni T, et al. Isolation of the TSLL1 and TSLL2 genes, members of the tumor suppressor TSLC1 gene family encoding transmembrane proteins. Oncogene. 2001; 20:5401–7. [PubMed: 11536053]

$watermark-text
$watermark-text
$watermark-text

12. Williams YN, Masuda M, Sakurai-Yageta M, Maruyama T, Shibuya M, Murakami Y. Cell adhesion and prostate tumor-suppressor activity of TSLL2/IGSF4C, an immunoglobulin superfamily molecule homologous to TSLC1/IGSF4. Oncogene. 2006; 25:1446–53. [PubMed: 16261159]
13. Ito A, Hagiyama M, Mimura T, et al. Expression of cell adhesion molecule 1 in malignant pleural mesothelioma as a cause of efficient adhesion and growth on mesothelium. Lab Invest. 2008; 88:504–14. [PubMed: 18332875]
14. Overmeer RM, Henken FE, Snijders PJ, et al. Association between dense CADM1 promoter methylation and reduced protein expression in high-grade CIN and cervical SCC. J Pathol. 2008; 215:388–97. [PubMed: 18498117]
15. Michels E, Hoebeeck J, De Preter K, et al. CADM1 is a strong neuroblastoma candidate gene that maps within a 3. 72 Mb critical region of loss on 11q23. BMC Cancer. 2008; 8:173. [PubMed: 18559103]
16. Raveh S, Gavert N, Spiegel I, Ben-Ze'ev A. The cell adhesion nectin-like molecules (Necl) 1 and 4 suppress the growth and tumorigenic ability of colon cancer cells. J Cell Biochem. 2009; 108:326–36. [PubMed: 19565570]
17. Giangreco A, Jensen KB, Takai Y, Miyoshi J, Watt FM. Necl2 regulates epidermal adhesion and wound repair. Development. 2009; 136:3505–14. [PubMed: 19783739]
18. Sakurai-Yageta M, Masuda M, Tsuboi Y, Ito A, Murakami Y. Tumor suppressor CADM1 is involved in epithelial cell structure. Biochem Biophys Res Commun. 2009
19. Biederer T, Sara Y, Mozhayeva M, et al. SynCAM, a synaptic adhesion molecule that drives synapse assembly. Science. 2002; 297:1525–31. [PubMed: 12202822]
20. Biederer T. Bioinformatic characterization of the SynCAM family of immunoglobulin-like domain-containing adhesion molecules. Genomics. 2006; 87:139–50. [PubMed: 16311015]
21. Dumur CI, Dechsukhum C, Ware JL, et al. Genome-wide detection of LOH in prostate cancer using human SNP microarray technology. Genomics. 2003; 81:260–9. [PubMed: 12659810]
22. Pietri T, Easley-Neal C, Wilson C, Washbourne P. Six cadm/SynCAM genes are expressed in the nervous system of developing zebrafish. Dev Dyn. 2008; 237:233–46. [PubMed: 18095341]
23. He TC, Zhou S, da Costa LT, Yu J, Kinzler KW, Vogelstein B. A simplified system for generating recombinant adenoviruses. Proc Natl Acad Sci U S A. 1998; 95:2509–14. [PubMed: 9482916]
24. Steiner MS, Zhang X, Wang Y, Lu Y. Growth inhibition of prostate cancer by an adenovirus expressing a novel tumor suppressor gene, pHyde. Cancer Res. 2000; 60:4419–25. [PubMed: 10969787]
25. Ctrnacta V, Ault JG, Stejskal F, Keithly JS. Localization of pyruvate:NADP+ oxidoreductase in sporozoites of Cryptosporidium parvum. J Eukaryot Microbiol. 2006; 53:225–31. [PubMed: 16872290]
26. Shah US, Dhir R, Gollin SM, et al. Fatty acid synthase gene overexpression and copy number gain in prostate adenocarcinoma. Hum Pathol. 2006; 37:401–9. [PubMed: 16564913]
27. Mao X, Seidlitz E, Ghosh K, Murakami Y, Ghosh HP. The cytoplasmic domain is critical to the tumor suppressor activity of TSLC1 in non-small cell lung cancer. Cancer Res. 2003; 63:7979–85. [PubMed: 14633730]
28. Hui AB, Lo KW, Kwong J, et al. Epigenetic inactivation of TSLC1 gene in nasopharyngeal carcinoma. Mol Carcinog. 2003; 38:170–8. [PubMed: 14639656]
29. Collard RL, Harya NS, Monzon FA, Maier CE, O'Keefe DS. Methylation of the ASC gene promoter is associated with aggressive prostate cancer. Prostate. 2006; 66:687–95. [PubMed: 16425203]
30. Narla G, DiFeo A, Yao S, et al. Targeted inhibition of the KLF6 splice variant, KLF6 SV1, suppresses prostate cancer cell growth and spread. Cancer Res. 2005; 65:5761–8. [PubMed: 15994951]
31. Li LC, Dahiya R. MethPrimer: designing primers for methylation PCRs. Bioinformatics. 2002; 18:1427–31. [PubMed: 12424112]
32. Davuluri RV, Grosse I, Zhang MQ. Computational identification of promoters and first exons in the human genome. Nat Genet. 2001; 29:412–7. [PubMed: 11726928]

33. Soejima K, Fang W, Rollins BJ. DNA methyltransferase 3b contributes to oncogenic transformation induced by SV40T antigen and activated Ras. Oncogene. 2003; 22:4723–33. [PubMed: 12879017]

34. Xiong Y, Dowdy SC, Podratz KC, et al. Histone deacetylase inhibitors decrease DNA methyltransferase-3B messenger RNA stability and down-regulate de novo DNA methyltransferase activity in human endometrial cells. Cancer Res. 2005; 65:2684–9. [PubMed: 15805266]

35. Zhao C, Lam EW, Sunters A, et al. Expression of estrogen receptor beta isoforms in normal breast epithelial cells and breast cancer: regulation by methylation. Oncogene. 2003; 22:7600–6. [PubMed: 14576822]

36. Huang Y, de la Chapelle A, Pellegata NS. Hypermethylation, but not LOH, is associated with the low expression of MT1G and CRABP1 in papillary thyroid carcinoma. Int J Cancer. 2003; 104:735–44. [PubMed: 12640681]

37. Lung HL, Leung Cheung AK, Xie D, et al. TSLC1 Is a Tumor Suppressor Gene Associated with Metastasis in Nasopharyngeal Carcinoma. Cancer Res. 2006; 66:9385–92. [PubMed: 17018592]

38. Mao X, Seidlitz E, Truant R, Hitt M, Ghosh HP. Re-expression of TSLC1 in a non-small-cell lung cancer cell line induces apoptosis and inhibits tumor growth. Oncogene. 2004; 23:5632–42. [PubMed: 15184878]

$watermark-text

$watermark-text

$watermark-text

$watermark-text
$watermark-text
$watermark-text

Fig.1A

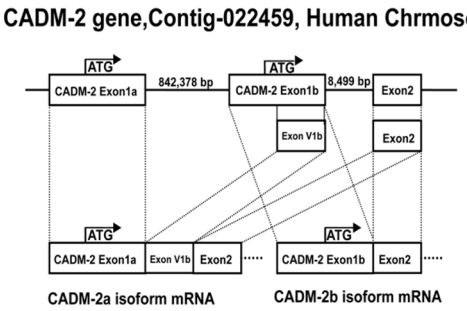

Fig.1B

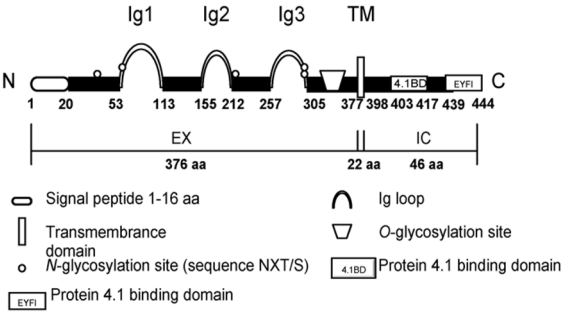

Figure 1.

A, A schematic representation of the untranslated regions of the human *CADM-2* gene illustrating the existence of separate promoters for each isoform. ***B,*** Schematic representation of putative domains of CADM-2a. EX, the extracellular domain; TM, the transmembrane domain; IC, the intracellular domain.

$watermark-text
$watermark-text
$watermark-text

Fig.2A

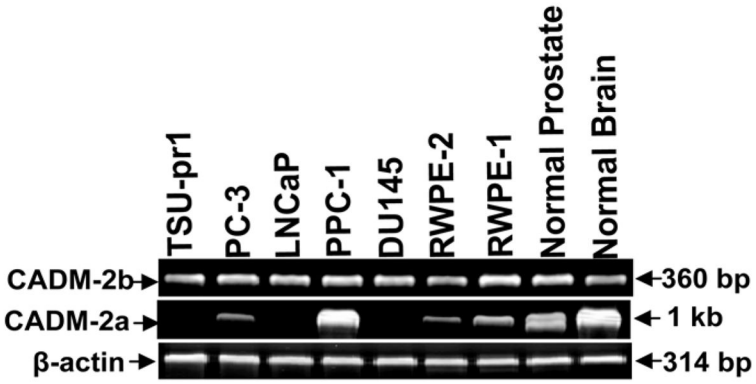

Fig.2B

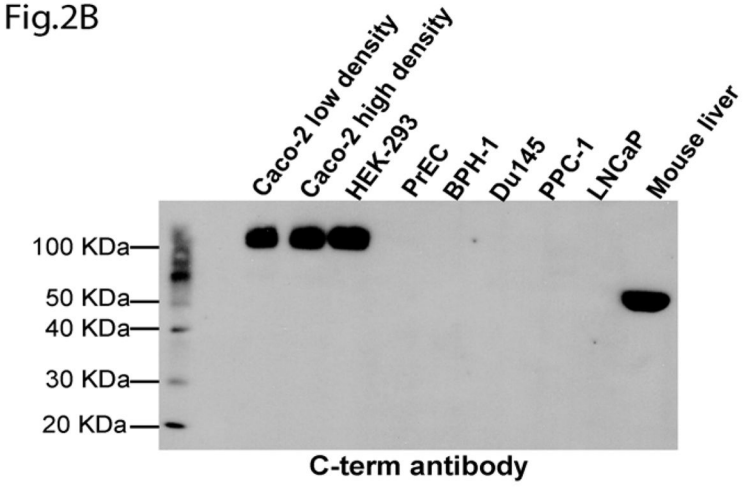

Figure 2.

A, Expression of *CADM-2a* and *CADM-2b* transcripts. Total RNA was extracted from human prostate cancer cell lines, a normal prostate epithelial cell line, and normal prostate and brain tissues. RT-PCR was performed using primer pairs that amplified a portion of each isoform specifically. Blot is representative of three independent experiments. ***B,*** Endogenous CADM-2 protein expression in several cell lines detected by C-term antibody.

$watermark-text

$watermark-text

$watermark-text

Fig.3A

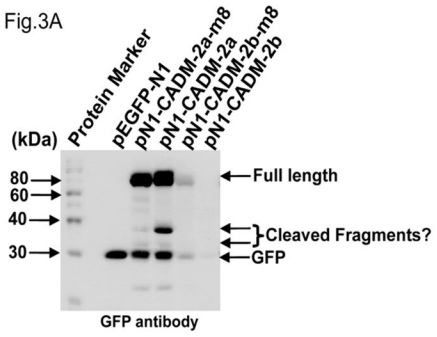

Fig.3B

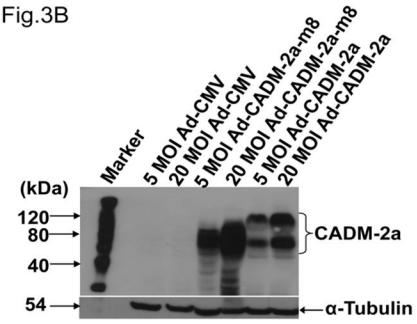

$watermark-text

$watermark-text

$watermark-text

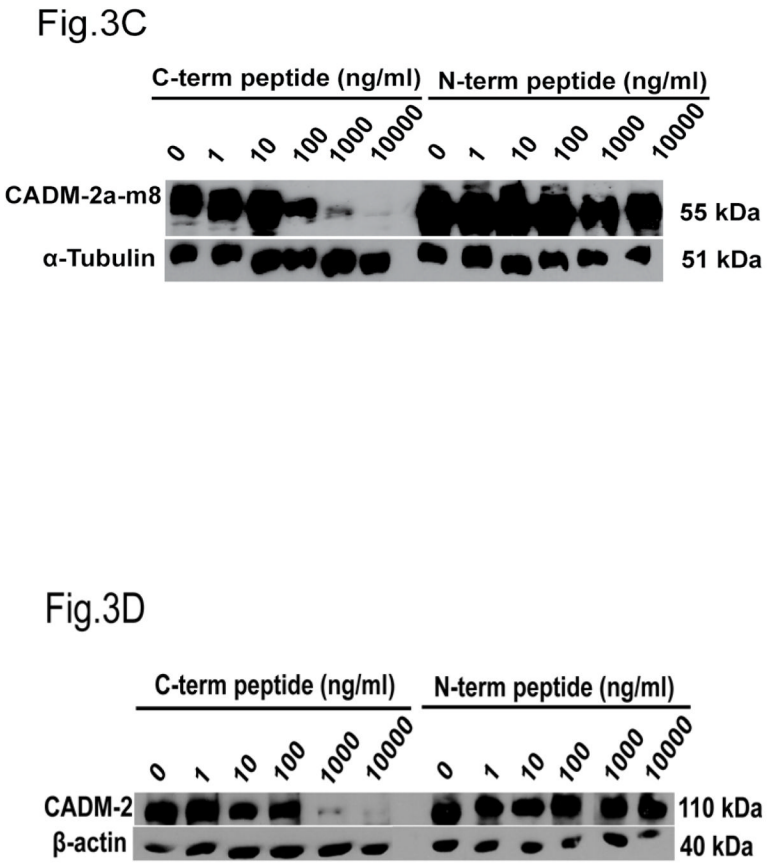

Figure 3.

Ecotopic expression of CADM-2 and its GFP fusion protein mediated by recombinant adenovirus or pEGFP-N1 vector, and determination of specificity of C-term antibody. ***A,*** CADM-2 GFP fusion protein expression of recombinant *CADM-2* isoforms transfected in HEK293 cells probed by GFP antibody. This blot is representative of three independent experiments. ***B,*** Western blot assay for adenoviral mediated CADM-2a expression detected by C-term antibody in prostate cancer cell line DU145. The expression of wild-type CADM-2a is correlated with adenoviral Mutiplicity Of Infections (MOIs). ***C,*** Peptide competition assay for determining the anti-CADM-2 C-term antibody specificity in Western blot analyses of extracts of DU145 transduced by Ad-CADM-2-m8 at MOI 5. Anti-CADM-2 was pre-incubated with serial homologous C-term peptide or heterologous N-term peptide. The heterologous peptide does not inhibit binding of anti-CADM-2 antibody to CADM-2 on the nitrocellulose membrane. Negative control: the secondary antibody was used without primary antibody (first band with 0 ug/ml). ***D,*** Peptide competition assay for determining the anti-CADM-2 C-term antibody specificity in Western blot analyses of endogenous CADM-2 expression in extracts of 293 cells. Therefore, C-term antibody is specific for both transfected and endogenous CADM-2 expression.

$watermark-text
$watermark-text
$watermark-text

Fig.4A

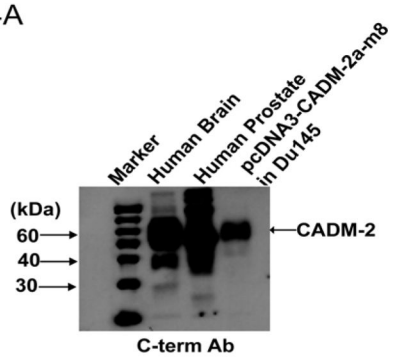

Fig.4B

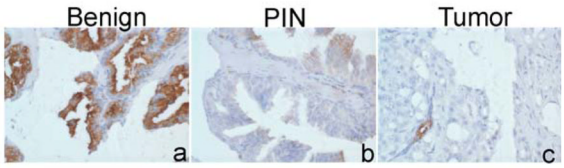

Figure 4.

A, Endogenous CADM-2 protein expression in normal brain and prostate tissue detected by C-term antibody. ***B,*** Endogenous CADM-2 protein expression in prostate specimens by C-term antibody. Prostate TMA slides were examined for CADM-2 protein expression by C-term antibody IHC: benign prostatic hyperplasia (a), PIN (b), Tumor (c), benign epithelium showed intense staining, while expression was decreased in PIN, and negligible in prostate cancer. Brown staining is indicative of CADM-2 protein expression (magnification × 60).

$watermark-text
$watermark-text
$watermark-text

Fig.5A

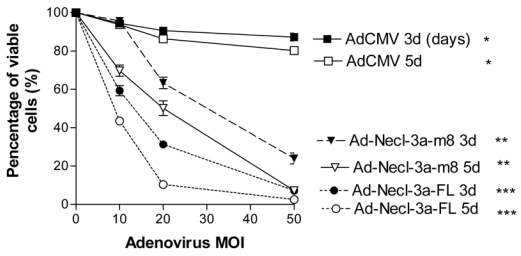

Fig. 5B

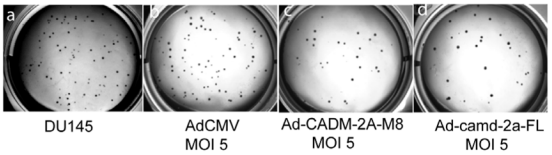

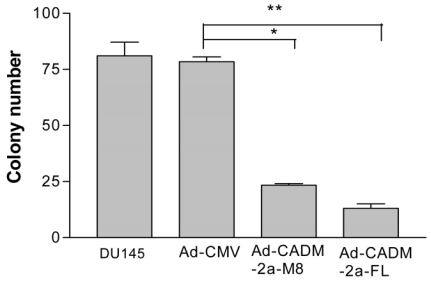

Figure 5.

CADM-2a functions as a tumor suppressor. ***A***, Effect of CADM-2a on DU145 cell proliferation. DU145 cells were infected with Ad-CADM-2a-FL, Ad-CADM-2A-m8 and Ad-CMV at various MOIs of 10, 20 or 50 for 3 or 5 days. DU145 cells were also treated with DMEM as a mock infection. The viability of cells was determined by MTT assay. Cell viability was expressed as the percentage of viable cells infected with adenoviral vector compared to the DMEM-treated control. There are significant difference between Ad-*CADM*-2a-FL (***) or Ad-*CADM*-2a -m8 group (**) and control viral group Ad-CMV (*) at day 3 or day 5 post-transduction respectively ($P < 0.01$). ***B***, CADM-2a attenuates anchorage-independent growth. Wells were coated with bottom agar and then overlayed with top agar containing DU145 cells transiently transduced with *(a)* parental DU145, *(b)* the empty vector Ad-CMV, *(c)* Ad-CADM-2a-*m8* and *(d)* Ad-CADM-2a-*FL* at moi 5. Colonies were observed under an IMT-2 inverted research microscope and photographed after 15 days. Colonies with more than 50 μm in diameter were counted. Each experiment was performed in triplicate wells and repeated three times. Results reported as mean ± standard deviation form 3 independent experiments. * and ** indicated that there are significant difference between Ad- CADM-2a-*m8* (* $P < 0.01$) or Ad-CADM-2a-*FL* (** $P < 0.01$) and Ad-CMV.

Fig.6A

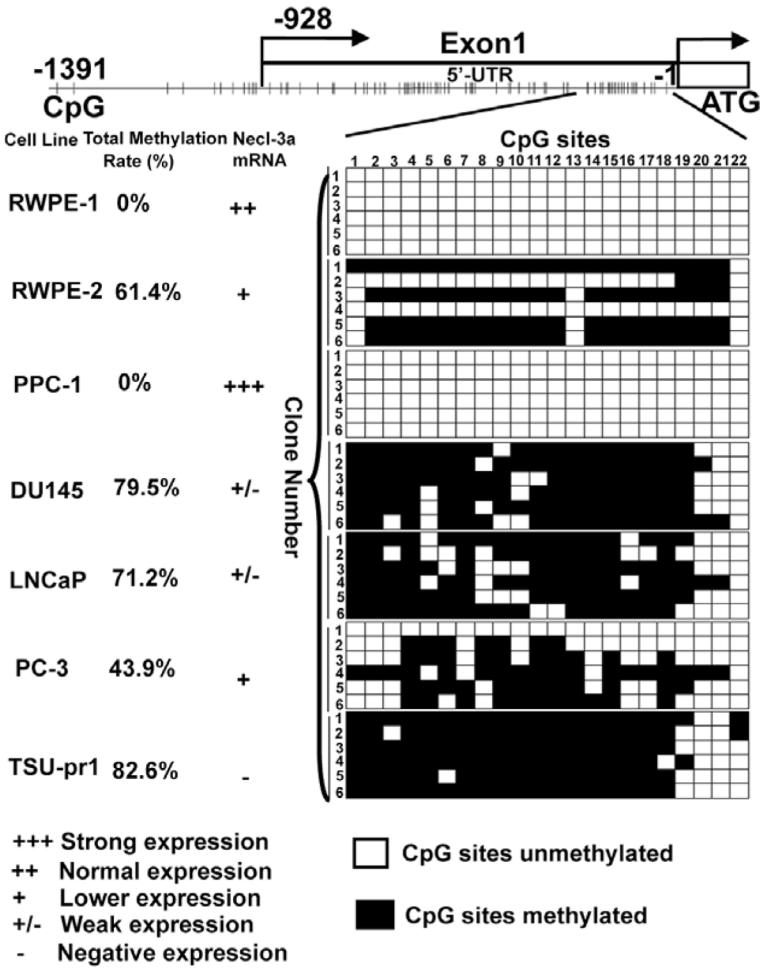

$watermark-text
$watermark-text
$watermark-text

$watermark-text

$watermark-text

$watermark-text

Fig.6B

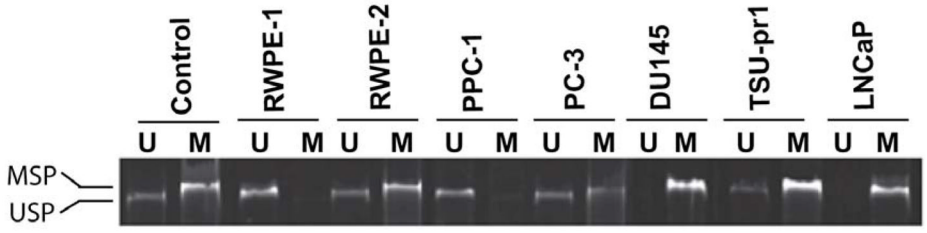

Fig.6C

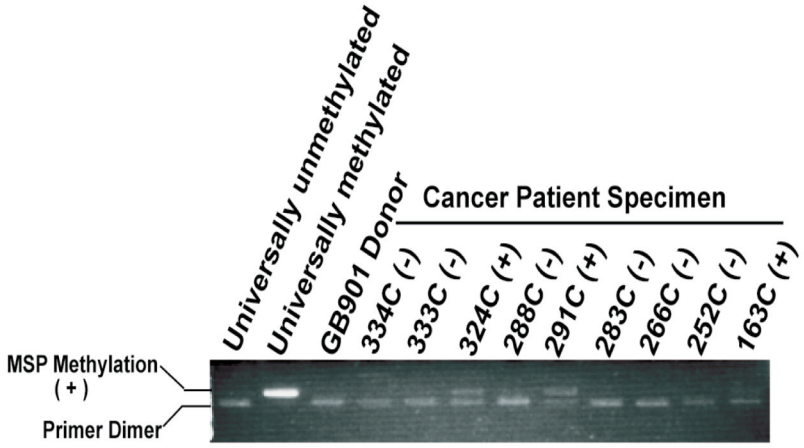

$watermark-text
$watermark-text
$watermark-text

Fig. 6D

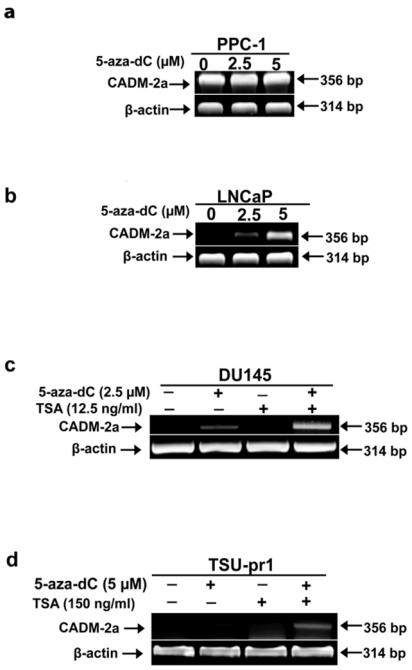

Figure 6.

A, Quantitation of *CADM-2a* promoter methylation in cell lines. The PCR products obtained after bisulfide treatment of genomic DNA were subcloned into T-A vectors. Six clones from each cell line were sequenced. Each square represents one of the 22 CpG dinucleotides in this DNA fragment. Methylated CpGs are shown as filled squares and unmethylated ones as blank squares. The overall percentage of methylated sites in the CpG island of *CADM-2a* from each cell line is given. ***B,*** Methylation-specific PCR analysis of cell lines. Bands in lanes labeled 'U' represent unmethylated DNA while bands in lanes labeled 'M' represent methylated DNA. Blot representative of three independent experiments. ***C***, MSP analysis of donor prostate epithelium and prostate cancer specimens from nine patients. ***D***, *CADM-2a* expression is reactivated by 5-aza-dC alone or in combination with TSA. **(*a* and *b*)** RT-PCR of *CADM-2a* mRNA from ***a,*** PPC-1 and ***b,*** LNCaP cells treated with increasing amounts of 5-aza-dC for 4 days. β-actin expression is constant and served as an internal control. **(*c* and *d*)** RT-PCR of *CADM-2a* or *β-actin* from ***c*** DU145 and ***d*** TSU-pr1 cells treated with 5-aza-dC and/or TSA for 4 days at the indicated concentration. Primers amplified a portion of specific to CADM-2a mRNA. Gel representative of three independent experiments.

$watermark-text $watermark-text $watermark-text

Table 1

CADM-2 protein expression in prostate tissue by tissue microarray.

Histology	*n*	Mean	*SD*	Median	25%	75%	*P* value
Adenocarcinoma	109	0.751	0.521	0.701	0.366	1.05	
NAT	42	2.089	0.621	1.866	1.667	2.833	*P*<.001 *
BPH	17	2.292	0.482	2.333	2.006	2.635	*P*<.001 *
PIN	38	2.282	0.476	2.165	1.917	2.75	*P*<.001 *
Donor	11	2.255	0.557	2.5	1.699	2.636	*P*<.001 *
Gleason 7	53	0.824	0.557	0.75	0.472	1.149	
Gleason <7	15	0.614	0.515	0.75	0.122	1	
Gleason >7	41	0.706	0.467	0.583	0.333	0.938	
Stage II	40	0.855	0.579	0.875	0.5	1.125	
Stage III	39	0.661	0.458	0.604	0.333	1	
Stage IV	29	0.748	0.53	0.688	0.371	1.138	

NOTE: TMA slides were stained for CADM-2 expression using a polyclonal antibody for CADM-2. Each core was then examined for expression and assigned a number from 0 to 4 dependent upon the intensity of CADM-2 immunostaining as determined by a pathologist. NAT: normal adjacent tissue; BPH: Benign prostatic hyperplasia; PIN: Prostate Intraepithelial Neoplasia.

* Significant difference from adenocarcinoma ($P < 0.001$).

$watermark-text $watermark-text $watermark-text

Table 2

Clinicopathological factors of nine prostate cancer patients and one normal donor.

Patient Number	PSA level	Gleason score	Pathological stage	Recurrence	MSP results
GB901 donor					No
163C	**4.1**	**9**	**T3bN1Mx**	**Yes**	**Yes**
252C	16.6	6	T1cN0Mx	Yes	No
266C	21.4	7	Unknown	No	No
283C	2.9	7	T3N0Mx	Yes	No
291C	**7**	**7**	**T3N1Mx**	**Yes**	**Yes**
288C	6	9	T3N2Mx	No	No
324C	**17**	**8**	**T2N0Mx**	**No**	**Yes**
333C	129	8	T3aN0Mx	No	No
334C	22.2	8	T3aN0Mx	No	No

PSA: prostate-specific antigen; MSP: methylation-specific PCR.